NeuroImage 85 (2014) 1040–1047

Contents lists available at ScienceDirect

NeuroImage

journal homepage: www.elsevier.com/locate/ynimg

Imaging artifacts induced by electrical stimulation during conventional fMRI of the brain

Andrea Antal [a,*], Marom Bikson [b], Abhishek Datta [b], Belen Lafon [b], Peter Dechent [c], Lucas C. Parra [b,1], Walter Paulus [a,1]

[a] Department of Clinical Neurophysiology, Georg-August University, 37075 Göttingen, Germany
[b] Department of Biomedical Engineering, The City College of The City University of New York, New York, NY, USA
[c] MR-Research in Neurology and Psychiatry, Georg-August University, 37075 Göttingen, Germany

ARTICLE INFO

Article history:
Accepted 17 October 2012
Available online 23 October 2012

Keywords:
fMRI
Post-mortem
Brain
tDCS
tACS
Modeling

ABSTRACT

Functional magnetic resonance imaging (fMRI) of brain activation during transcranial electrical stimulation is used to provide insight into the mechanisms of neuromodulation and targeting of particular brain structures. However, the passage of current through the body may interfere with the concurrent detection of blood oxygen level-dependent (BOLD) signal, which is sensitive to local magnetic fields. To test whether these currents can affect concurrent fMRI recordings we performed conventional gradient echo-planar imaging (EPI) during transcranial direct current (tDCS) and alternating current stimulation (tACS) on two post-mortem subjects. tDCS induced signals in both superficial and deep structures. The signal was specific to the electrode montage, with the strongest signal near cerebrospinal fluid (CSF) and scalp. The direction of change relative to non-stimulation reversed with tDCS stimulation polarity. For tACS there was no net effect of the MRI signal. High-resolution individualized modeling of current flow and induced static magnetic fields suggested a strong coincidence of the change EPI signal with regions of large current density and magnetic fields. These initial results indicate that (1) fMRI studies of tDCS must consider this potentially confounding interference from current flow and (2) conventional MRI imaging protocols can be potentially used to measure current flow during transcranial electrical stimulation. The optimization of current measurement and artifact correction techniques, including consideration of the underlying physics, remains to be addressed.

Introduction

Transcranial stimulation with weak currents, including transcranial direct current stimulation (tDCS) and transcranial alternating current stimulation (tACS), are able to modify a range of neuropsychiatric disorders, facilitate stroke rehabilitation, and enhance cognitive function (for reviews see e.g.: (Antal et al., 2011a; Jacobson et al., 2012; Nitsche and Paulus, 2011; Reis and Fritsch, 2011). To achieve optimal outcomes one may wish to target specific brain regions by carefully selecting electrode position and size (Datta et al., 2011; Dmochowski et al., 2011). Predicting the effectiveness of such targeting relies thus far on computational models of current flow or is based on imaging of physiological responses in the brain. For this purpose, positron emission tomography (PET) scanning can be readily combined with electrical stimulation (Lang et al., 2005). However, to avoid radiation concerns it is preferable and more common to use functional magnetic resonance imaging (fMRI) (Antal et al., 2011b; Holland et al., 2011). fMRI after or during electrical stimulation provides information of regional brain activation (Kwon et al., 2008) and these, in turn, can be correlated with behavioral outcomes. However, the precise relationship between stimulation montage, concurrent tasks, and blood oxygen level-dependent (BOLD) signal remain unresolved, presumably reflecting both the role of connectivity, (Polania et al., 2011), the complex (non-linear) response of neuron to electrical stimulation, and the further non-monotonic rectifying transformation to BOLD or arterial spin labeling (ASL) signal (Zheng et al., 2011). The role of current flow itself producing an artifact or distortion of the BOLD signal has thus far not been considered. This is important, considering that applied currents generate magnetic fields and these may interfere with the MRI imaging sequences which rely on carefully controlled magnetic field distributions.

Computational models that predict current flows in the brain show that conventional electrode montages lead to broadly distributed electric fields across cortex with idiosyncratic "hot-spots" of stimulation (Datta et al., 2010, 2011; Salvador et al., 2010). Despite the promise of these models in the design and interpretation of clinical and non-clinical studies, direct validation has remained elusive. Recent efforts

* Corresponding author at: Department of Clinical Neurophysiology, Georg-August University, Robert-Koch-Str. 40, 37075 Göttingen, Germany. Fax: +49 551 398126.
E-mail address: aantal@gwdg.de (A. Antal).
[1] These authors contributed equally.

1053-8119/$ – see front matter © 2012 Elsevier Inc. All rights reserved.
http://dx.doi.org/10.1016/j.neuroimage.2012.10.026

have correlated plastic changes evidenced by fMRI (Halko et al., 2011) and clinical outcome (Datta et al., 2011) to patient-specific electric field modeling respectively. Specialized MRI sequences have been proposed in the past to directly measure current flow (e.g. (Joy et al., 1989; Scott et al., 1991, 1992)), but the feasibility of these techniques for low-intensity currents and using conventional scanning remains unclear.

The aim of this study was to differentiate between real physiological BOLD changes induced by tDCS and possible concurrent signal artifacts arising from the current flow in tissue. We suspected that conventional fMRI, specifically, echo-planar imaging (EPI), may be subject to artifacts resulting from the local magnetic fields generated by the applied electric currents. To test this, we imaged the brain of post-mortem subjects using a conventional EPI sequence. Evidently, functional hemodynamic changes in brain activity are absent in these recordings and any detected signal must be the result of the applied currents. Our results demonstrate (1) the feasibility of current imaging using low-intensity stimulation and conventional imaging sequences and (2) the requisite to consider current flow "artifact" when imaging physiologic responses to brain stimulation, in particular if localized in the CSF.

Methods

Subjects

Two female subjects (78 and 86 years old), who deceased 1 and 5 days before the measurements, were included in the experiment. Both of the subjects passed away due to non-neurological or non-psychiatric diseases. The bodies were kept in a cold storage and were not otherwise preserved. The experimental procedure was approved by the Ethical Committee of the University of Göttingen.

Transcranial direct current stimulation (tDCS)

Direct and alternating currents with 1 mA intensity were applied via a pair of square rubber electrodes (7 × 5 cm), manufactured to be compatible with the MR-scanner environment. The electrodes were equipped with 5.6 kOhm resistors in each wire to avoid sudden temperature increases due to induction voltages from radio frequency pulses. They were connected to a specially developed battery-driven stimulator (MR Plus, NeuroConn GmbH, Ilmenau, Germany) outside the magnet room via a cable running through a radio frequency filter tube in the cabin wall. Two filter boxes were placed between the stimulator and the electrodes (Antal et al., 2011b).

In both subjects one electrode was placed over the C3 electrode position according to the 10–20 electrode placement system. The return electrode was placed over the contralateral orbit. In the second subject an additional montage incorporated electrodes placed over the occipito-temporo-parietal junction, centred between O1–P3 and O2–P4, respectively.

Three different stimulation conditions were applied: anodal and cathodal tDCS and 40 Hz sinusoidal tACS. The stimulation paradigm was implemented as a block design with stimulation ON and OFF for blocks of 20 s each, and repeated eight times.

Functional magnetic resonance imaging (fMRI)

MRI recordings were obtained at 3 T (Magnetom TIM Trio, Siemens Healthcare, Erlangen, Germany) using a standard eight-channel phased array head coil. Subjects were placed supine inside the magnet bore. Initially, anatomic images based on a T1-weighted 3D turbo fast low angle shot (FLASH) MRI sequence at 1 mm^3 isotropic resolution were recorded (repetition time (TR) = 2250 ms, inversion time: 900 ms, echo time (TE) = 3.26 ms, flip angle: 9°). To keep with common practice in fMRI, we used a multislice T2*-sensitive gradient-echo echo-planar imaging (EPI) sequence (TR = 2000 ms, TE = 36 ms, flip angle 70°) at 2 × 2 mm^2 resolution. Twenty-two consecutive sections at 4 mm thickness in an axial-to-coronal orientation roughly parallel to the intercommisural plane were acquired, covering the brain areas of interest. For comparison, data was also collected from one healthy subject during a conventional finger tapping task, without stimulation. The block design for periods of finger tapping as well as the data acquisition were identical.

Data analysis

EPI magnitude was analysed with "BrainVoyagerQX" using standard procedures (version 1.10.2., Brain Innovation, Maastricht, The Netherlands). Raw magnitude data without any preprocessing were co-registered to the anatomical dataset. Generalized linear model (GLM) analysis was applied for each stimulation condition and each subject separately with stimulation ON/OFF as binary regression variable. We report both the z-scores (sub-cranial structures, Figs. 1 and 2) as well as raw correlation values, r, of the EPI magnitude signal with the binary regression variable (Fig. 3). The conventional measure of significance in fMRI is the z-score, which quantifies the mean difference between the ON/OFF conditions divided by the variability within conditions. However, variability here is not due to physiological fluctuations in resting BOLD as with an in-vivo recording, but rather, it is purely due to equipment noise, making this conventional normalization here perhaps less meaningful. Correlation, r, instead, is not normalized by noise and directly measures signal magnitude. Specifically, it measures the mean difference between the EPI signal during the ON minus the OFF condition (scaled by 0.25 if the regression variable is 1/0 for the ON/OFF periods respectively). This measure can directly be compared in magnitude and sign to values obtained during in-vivo recordings. In Fig. 3 only significant correlations are shown ($p < 0.001$, df = 168, with Bonferroni correction). Following standard practice to remove non-tissue voxels, activities with raw signal magnitudes below a background noise-floor value of 100 were excluded from analysis. On Figs. 1 and 2 only t-values are shown ($q(\mathrm{FDR}) = 0.05$).

To estimate signal magnitudes (Fig. 4), raw EPI magnitude data was also analysed (in MATLAB) with minimal processing: mean and linear trend over the $n = 170$ frames were removed; voxels with signal magnitudes below 100 were excluded as before; and frames with head movement artifacts in the finger tapping task were also excluded (mean deviation across voxels above 17). For comparison, note that median EPI magnitude in tissue was in the range of 700–1000.

Computational model

Current density computation

The voltage distribution in a volume during constant current flow in a resistive medium is governed by the Laplace equation. The solutions are valid to very good approximation also for low frequency AC currents (<1 kHz). The two post-mortem MRI datasets, as collected during the stimulation experiment, were demarcated into compartments representing the skin, skull, CSF, gray matter, white matter, and air using a combination of automated and manual segmentation routines (Datta et al., 2011). 5 × 7 cm size stimulation pads were imported as CAD models and positioned within the image data. Volumetric meshes were subsequently generated from the compartments (SIMPLEWARE Ltd, Exeter, UK) and imported to a commercial finite element solver (COMSOL Inc, MA, USA). Standard tissue conductive properties and boundary conditions were assigned as described previously (Bikson et al., 2012; Datta et al., 2011) and the classical Laplace equation was solved. Figs. 1 and 2 show the sub-cranial magnitude of current density in CSF, gray and white matter regions for subject 1 and 2 respectively. The complete data set is made available through the CCNY BONSAI interface (www.neuralengr.com/BONSAI).

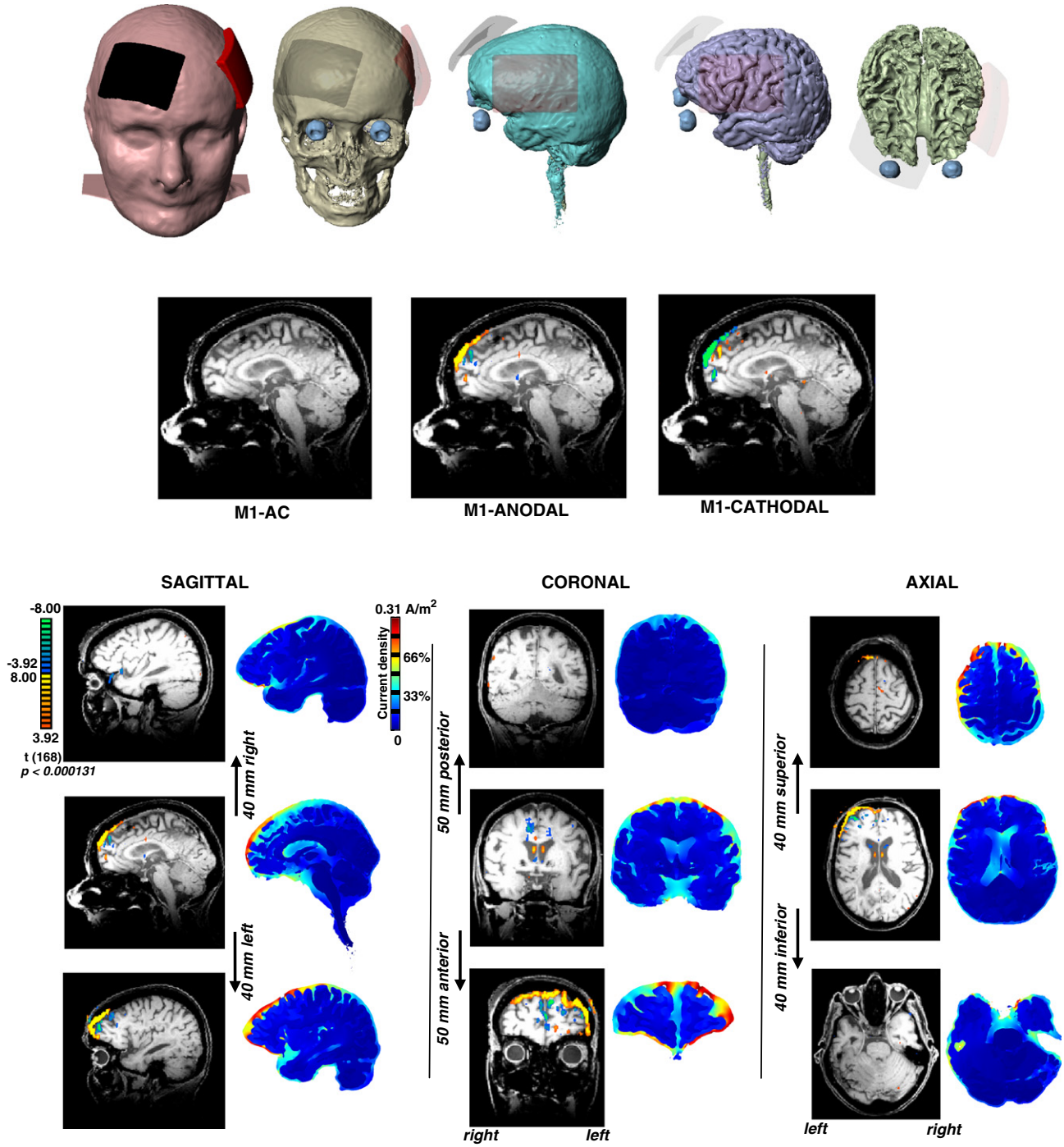

Fig. 1. Transcranial direct current stimulation (tDCS) in a post-mortem subject 1 produces significant polarity specific gradient-EPI magnitude signal. Top row: Reconstructed masks of main tissue from 86 year old female subject with tDCS electrode montage shown. Middle: EPI t-score during AC, M1 anodal, and M1 cathodal stimulation. Bottom: Sections of EPI z-score and current flow density maps predicted using FEM analysis of M1 anodal tDCS.

Magnetic field computation

Static currents produce a static magnetic field following the Biot-Savart law. We implemented the required integration of current density over the entire head volume as a 3D convolution in MATLAB. Magnetic fields were computed in vertical and both transverse directions, but we present here the results only for the vertical direction. B_z, depends on the electric current densities, J_x, J_y, in the transverse directions as: $B_z(\boldsymbol{r}) = J_x(\boldsymbol{r})*h_y(\boldsymbol{r}) - J_y(\boldsymbol{r})*h_x(\boldsymbol{r})$, where '*' represents a 3D convolution with the 3D point-spread function $\boldsymbol{h}(\boldsymbol{r}) = \boldsymbol{r}/|\boldsymbol{r}|$^3, and $\boldsymbol{r}$ represents a location in the 3D space. Fig. 3 shows magnetic field and the current density through the whole head in 3 exemplary slices.

Results

Imaging using a standard fMRI sequences and signal processing (see Methods) during tDCS in post-mortem subjects produced the largest EPI signals between the electrodes, with maximum intensities in the cerebrospinal fluid (CSF) and scalp (Figs. 1 and 3). Reversing the direction of current flow resulted in a signal with similar spatial

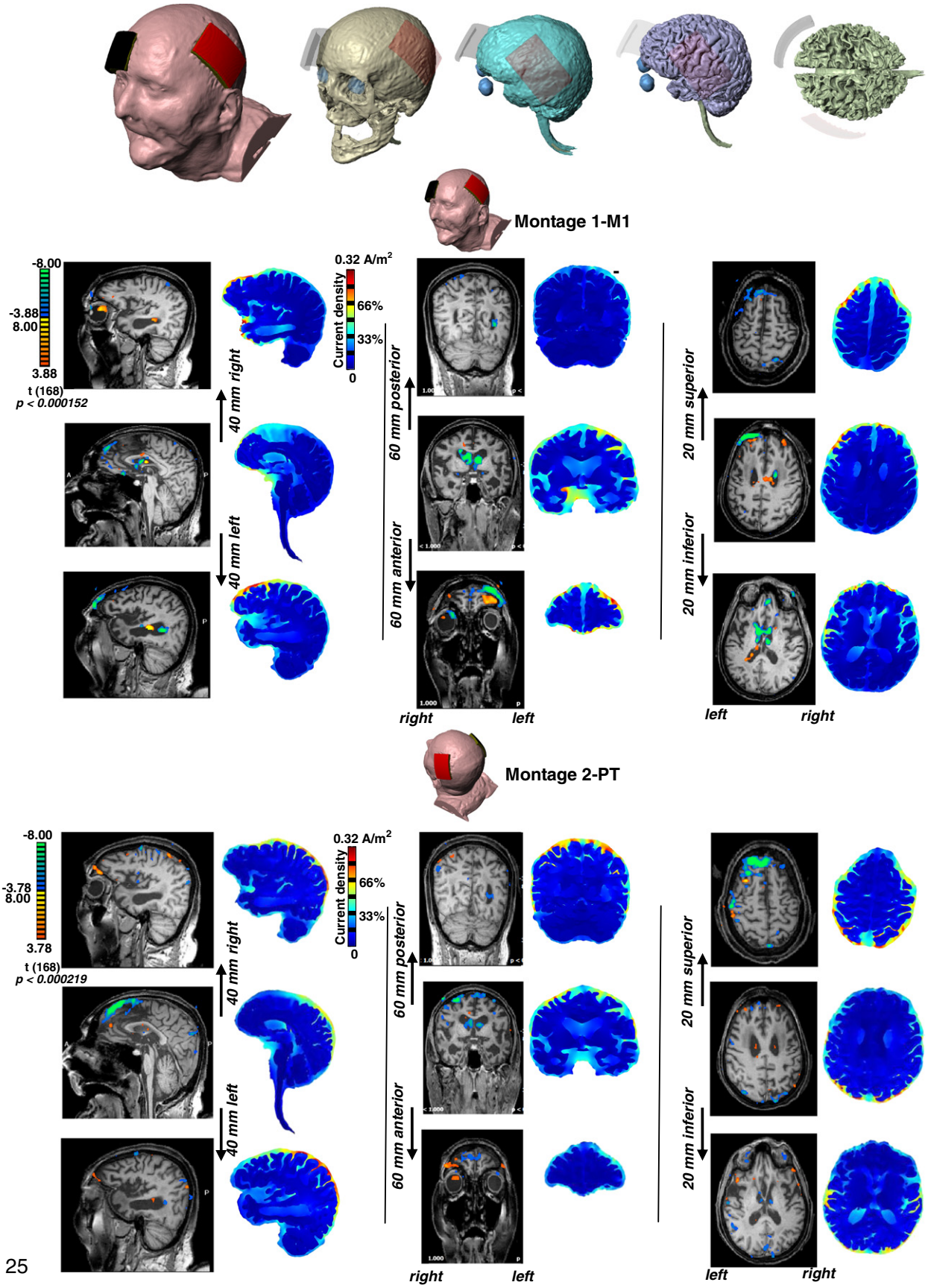

Fig. 2. Transcranial direct current stimulation (tDCS) in a post-mortem subject 2 produces montage-specific polarity specific gradient-EPI magnitude signal. Likewise montage-specific current clustering is also predicted by the FEM model. Top row: Reconstructed masks of main tissue from a 78 year old female subject with one tDCS electrode montage shown. Middle and bottom rows: Sections of EPI t-score and current flow density maps predicted using FEM analysis for both tested montages: M1 anodal (middle) and PT anodal (bottom).

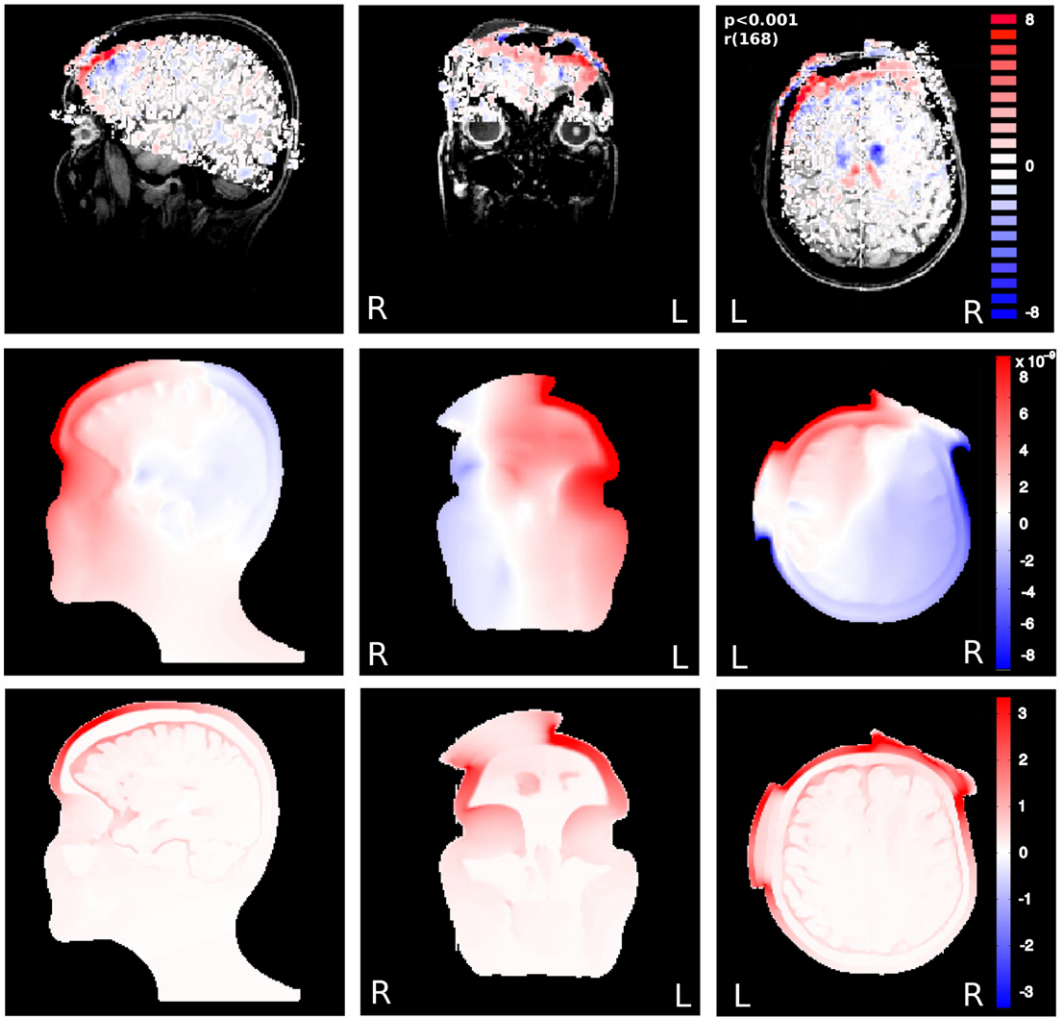

Fig. 3. Comparison of correlation, *r*, with predicted magnetic field in Z-axis and current density over the entire head including scalp. Top: Correlation *r* as reported by fMRI analysis software (BrainVoyagerQX). Middle: Predicted B_z field in units of Tesla (10^{-9} T). Bottom: Predicted current density intensity in the whole head in units of A/m^2. Stimulation intensity was 1 mA as in the post-mortem experiment.

profile but inverted polarity (Fig. 1, middle row). For stimulation with AC currents, which had a net-zero charge, no signal was detected.

High-resolution finite element method (FEM) modeling of current flow based on the individual anatomy obtained from the subjects' MRI led to local maxima in both superficial CSF and ventricles (Figs. 1–3), consistent with previous models. These areas of maximal current flow coincided with large EPI signals. In both the EPI and current model, the distributions were montage dependent (Figs. 1 and 2). Note that Fig. 1 only shows current density magnitude, and not polarity. While current direction reverses when stimulation polarity is reversed, the polarity of simulated current flows did not correspond to the directions of change observed in the EPI signal.

We suspected that polarity reversals may be due to reversal of magnetic field orientation generated by the applied currents, in particular the field in the vertical direction (B_z). The polarity of the field corresponds in sign to the EPI signal changes (Fig. 3). Upwards pointing B_z fields coincide largely with increased EPI signal, and downward pointing fields with decreased EPI signal. However, the correspondence between EPI signal and either current flow or B_z field is not complete. In particular, the reversal in EPI signal in the ventricles is not reproduced by either the estimated magnetic or the estimated electric fields.

To estimate the magnitude of the EPI artifact relative to a normal physiological BOLD response we compared the raw EPI signal (see Methods) during tDCS to a conventional finger tapping task using the identical imaging sequence with the identical block design (Fig. 4). The variability of overall activity is larger during the physiological BOLD response as compared to the post-mortem recordings by only a factor of 2, indicating that measurement noise of the equipment itself is significant in size (BOLD SNR of approximately 6 dB). To mitigate these high noise levels, it is customary to average the activity over many frames. The effect size of tDCS alone (no BOLD) – measured as the mean difference between the ON and OFF periods – is comparable in magnitude to the effect sizes of the physiological BOLD response during finger tapping (approximately 1/2 or −6 dB) – thus, by no means negligible.

Discussion

Changes in the EPI signal, as conventionally acquired in fMRI, in two post-mortem subjects were maximal on the scalp and in CSF. The locations of highest intensity broadly coincide with high-resolution estimates of electric current distributions and the resulting magnetic B_z fields. The prevalence of artifact signal on scalp and CSF was consistent with higher current densities resulting from the high conductivity of these structures. Consistent with model predictions, the peak of activation is not simply under the stimulating electrode, as often naively

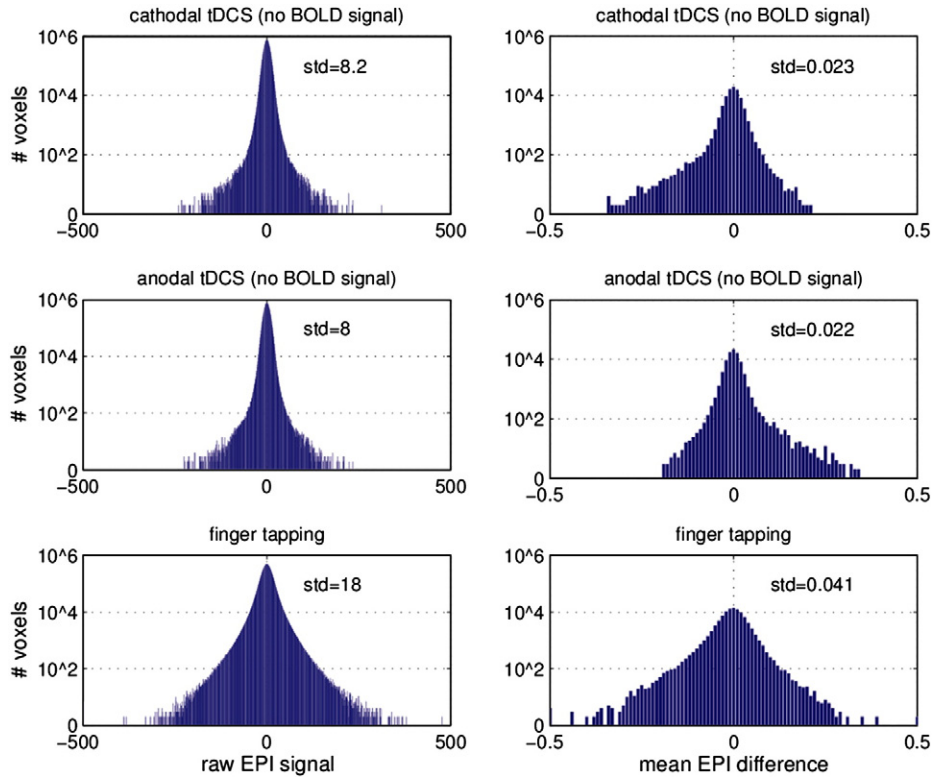

Fig. 4. Comparison of EPI signal during tDCS (post-mortem, no BOLD signal) with physiological BOLD response during conventional finger tapping experiment. Left: Histogram of raw EPI signal across voxels and time (only mean and linear trend have been removed). As a reference, the median EPI signal in tissue for cathodal tDCS, anodal tDCS and finger tapping was 929, 930, and 765 respectively. Right: Histogram of mean EPI difference across voxels (difference between ON/OFF and tapping/no-tapping respectively).

assumed, but rather between electrodes as suggested by computational models.

MRI is dependent on the generation of magnetic fields by the scanner, but in addition, it is well established that MRI signal is sensitive to local variations in static magnetic field generated by current flow in the sample. Specifically the B_z component of the magnetic field which is parallel with the static field is known to linearly change phase and magnitude profiles (Scott et al., 1991). This inherent sensitivity can be exploited to measure magnetic fields generated by electrical current flowing through human tissues generated either endogenously by neuronal activity (Bodurka and Bandettini, 2002; Konn et al., 2003; Xiong et al., 2003) or exogenously applied and thus dependent on electrode configuration and waveform (AC, DC). As a first approximation, we compared the magnitude signal change (captured in the correlation r) with predicted B_z field (Fig. 3); though polarity reversals and qualitative correlation were observed, further analysis explicitly considering imaging physics is warranted.

Initial studies (Scott et al., 1991, 1992) characterized "current flow imaging" in phantoms and tissue using spin-echo or gradient-echo with EPI sequences, and using pulsed currents (synchronized to the imaging sequence) and later static (DC) currents (Bodurka et al., 1999; Wojtczyk et al., 2011). These studies confirm that inhomogeneous magnetic fields resulting from current flow produce "distortions" in the MRI signal that can, in turn, quantitatively predict current density in the volume ("magnetic inverse problem"). The sensitivity of phase- and magnitude-based MR current measurements to scanner intensity (1.5 or 3 T) and to additional sequences (FLASH, trueFISP; MAGSUS) was explored by Wojtczyk et al. (2011). The present study demonstrates that imaging of low-intensity, well tolerated, transcranial current flow using standard fMRI sequences and protocols is possible, e.g. using gradient-echo echo-planar imaging. The magnitude of the artifact signal resulting from the electric current alone was approximately 1/2 of a typical physiological BOLD response. The stimulation-induced signal was not described by previous reports using conventional concurrent tDCS-fMRI measurements (Kwon et al., 2008); however, in our initial tDCS-FMRI studies we observed some artifacts initiated the present study.

Additional efforts are under way to measure current directly in the scanner such as the use of low-field nuclear magnetic resonance imaging (Hofner et al., 2011) and magnetic resonance electrical impedance tomography (MREIT) (Kim et al., 2007, 2008). Here we have intentionally analyzed only the magnitude images, since this is the standard procedure used for BOLD responses. Future studies should include an analysis of both EPI magnitude and phase images.

An important feature of the EPI magnitude differences observed here is their reversal with changing DC polarity. Equally important is the absence of an average EPI magnitude difference during AC stimulation as compared to no stimulation. Together this might suggest that the signal reverses with equal strength for opposing polarities so that AC produces no net signal. Thus, fMRI signal artifact from current flow may be a lesser concern for studies using tACS, though caution and further sequence-specific confirmation is warranted.

In conventional fMRI, blood oxygenation changes are only indirectly inferred from the varying magnetic susceptibility of oxygenated versus de-oxygenated blood. These changes in susceptibility affect the T2* relaxation time constant and thus the signal magnitude. In gradient-echo EPI imaging non-uniform magnetic fields can also alter the effective T2* leading to imaging artifacts (Howseman et al., 1999). Here, the magnetic field distributions resulting from the applied currents during transcranial stimulation are non-uniform (Fig. 3). This should lead to a reduction in T2* and thus a reduction of signal magnitude. However, if this was the source of the EPI magnitude changes observed here, one would not expect a reversal (increase/decrease) with changing current polarity. Further, one would expect the effect to also be present for AC stimulation, which has the same field inhomogeneities. B_z inhomogeneities during the EPI can also cause phase shifts in the resonance signal,

and these shifts reverse direction with opposite polarities. When phase is used for spatial encoding, this leads to image distortions, which should reverse in direction with changing current polarity. In this view, it is possible that the effects observed here on signal magnitude results from the difference between a spatially distorted and an undistorted EPI image in the ON/OFF conditions. An alternative explanation for the observed effects is that the applied fields interfere with the automatic shimming procedures of modern MRI machines. Shimming aims to achieve a uniform field and thus non-uniformities may lead to systematic changes in the MRI acquisition parameters (e.g. resonance frequency) which would reverse with field polarity.

We did not see any evidence of currents being induced in the electrodes or wires. It is possible that Eddy currents were induced by the MRI imaging sequence within the electrode material itself, but these would have been the same in the ON and OFF periods. By taking the difference between the two, as we did, any such effects would be canceled. We used a MRI-compatible stimulator (MR Plus, NeuroConn), which is designed to minimize currents in the wires and which explicitly controls current flow by means of a current-control circuit. To be certain that no currents are induced in the stimulation loop, future studies should also include a condition where the electrodes are disconnected from the stimulator.

There is increased interest to combine concurrent electrical stimulation and fMRI. In our hands, neither anodal nor cathodal tDCS, applied over the M1, induced a detectable BOLD signal change in normal subjects at rest (Antal et al., 2011b). However, during finger tapping anodal tDCS resulted in a decrease in the BOLD response in the supplementary motor area (SMA). Effects of anodal tDCS at M1 across broad brain regions, including an increase in the BOLD signal at left SMA and at the right posterior parietal cortex, have also been reported (Kwon et al., 2008). Zheng et al. (2011) using arterial spin labeling have demonstrated that both anodal and cathodal tDCS resulted in a significant increase in regional CBF (rCBF) under the electrode with anodal tDCS causing an increase three times higher than cathodal tDCS. tDCS-induced rCBF changes were observable in a widespread network, specifically involving contralateral motor-related cortical areas. Here we used the same conventional imaging sequence and brain stimulation methods as compared to some of these earlier studies, and observed strong signals despite the obvious absence of any real hemodynamic response.

Tissue properties and the CSF ion and protein concentration change in post-mortem subjects, for example as result of cell degeneration, disruption of brain barrier function, dehydration, or temperature (Li et al., 1968; Wendel and Malmivuo, 2006). Although the flow velocity of the ions in the CSF at the applied current intensity is very low, it cannot be ruled out that the application of tDCS during functional imaging induces some physical movement of CSF, which could in turn produce changes in EPI signal magnitude.

Under current control, overall resistance change would influence electric field but not average current density. Only significant change in relative resistivity (i.e. resistivity ratios) would affect current distributions. Gross anatomical changes typical with aging (notably changes in CSF thickness) and following death were taken into account, since we generated subject-specific models based on high-resolution anatomical scans collected in the same session. There is no evident a priori reason to assume the physics of current imaging would be altered compared to healthy subjects. Further refinement and quantification of the magnetic inverse problem for current imaging may eventually allow direct validation of modeling assumptions and techniques (Bikson and Datta, 2012). For instance, it may allow validation of the recently reported phenomenon that in EEG recordings current flow changes with subject's position as a result of changes in CSF thickness (Rice et al., 2013).

In summary, using a conventional EPI imaging sequence one can detect signals which coincide with regions of high current flow and resultant B_z fields. The exact relationship of these signals to the underlying current distributions remains to be developed based on physical principles. However, polarity reversal with DC stimulation and absence of signal in the case of AC stimulation encourages us to assume that these signals can in principle be inverted to recover electric field magnitudes within the brain. The signal already validates some basic observations made with computational models of current flow, most notably, that maximum intensity is achieved not underneath large electrode pads but in regions between the electrodes. Finally, functional MRI studies with concurrent direct current stimulation should apply utmost care when interpreting the data due to signal artifacts that may result from the magnetic field inhomogeneities generated by the applied currents; when "BOLD signals" occur in the CSF, particular attention is warranted.

Acknowledgments

We would like to thank Zsolt Turi for his technical assistance, Alexander Opitz for the theoretical comments and Truman Brown for highlighting the potential influence of shimming.

References

Antal, A., Paulus, W., Nitsche, M.A., 2011a. Electrical stimulation and visual network plasticity. Restor. Neurol. Neurosci. 29, 365–374.
Antal, A., Polania, R., Schmidt-Samoa, C., Dechent, P., Paulus, W., 2011b. Transcranial direct current stimulation over the primary motor cortex during fMRI. Neuroimage 55, 590–596.
Bikson, M., Datta, A., 2012. Guidelines for precise and accurate computational models of tDCS. Brain Stimul. 5, 430–431.
Bikson, M., Rahman, A., Datta, A., Fregni, F., Merabet, L., 2012. High-resolution modeling assisted design of customized and individualized transcranial direct current stimulation protocols. Neuromodulation 15, 306–315.
Bodurka, J., Bandettini, P.A., 2002. Toward direct mapping of neuronal activity: MRI detection of ultraweak, transient magnetic field changes. Magn. Reson. Med. 47, 1052–1058.
Bodurka, J., Jesmanowicz, A., Hyde, J.S., Xu, H., Estkowski, L., Li, S.J., 1999. Current-induced magnetic resonance phase imaging. J. Magn. Reson. 137, 265–271.
Datta, A., Bikson, M., Fregni, F., 2010. Transcranial direct current stimulation in patients with skull defects and skull plates: high-resolution computational FEM study of factors altering cortical current flow. Neuroimage 52, 1268–1278.
Datta, A., Baker, J.M., Bikson, M., Fridriksson, J., 2011. Individualized model predicts brain current flow during transcranial direct-current stimulation treatment in responsive stroke patient. Brain Stimul. 4, 169–174.
Dmochowski, J.P., Datta, A., Bikson, M., Su, Y., Parra, L.C., 2011. Optimized multi-electrode stimulation increases focality and intensity at target. J. Neural Eng. 8, 046011.
Halko, M.A., Datta, A., Plow, E.B., Scaturro, J., Bikson, M., Merabet, L.B., 2011. Neuroplastic changes following rehabilitative training correlate with regional electrical field induced with tDCS. Neuroimage 57, 885–891.
Hofner, N., Albrecht, H.H., Cassara, A.M., Curio, G., Hartwig, S., Haueisen, J., Hilschenz, I., Korber, R., Martens, S., Scheer, H.J., Voigt, J., Trahms, L., Burghoff, M., 2011. Are brain currents detectable by means of low-field NMR? A phantom study. Magn. Reson. Imaging 29, 1365–1373.
Holland, R., Leff, A.P., Josephs, O., Galea, J.M., Desikan, M., Price, C.J., Rothwell, J.C., Crinion, J., 2011. Speech facilitation by left inferior frontal cortex stimulation. Curr. Biol. 21, 1403–1407.
Howseman, A.M., Thomas, D.L., Pell, G.S., Williams, S.R., Ordidge, R.J., 1999. Rapid T2* mapping using interleaved echo planar imaging. Magn. Reson. Med. 41, 368–374.
Jacobson, L., Koslowsky, M., Lavidor, M., 2012. tDCS polarity effects in motor and cognitive domains: a meta-analytical review. Exp. Brain Res. 216, 1–10.
Joy, M., Scott, G., Henkelman, M., 1989. In vivo detection of applied electric currents by magnetic resonance imaging. Magn. Reson. Imaging 7, 89–94.
Kim, H.J., Lee, B.I., Cho, Y., Kim, Y.T., Kang, B.T., Park, H.M., Lee, S.Y., Seo, J.K., Woo, E.J., 2007. Conductivity imaging of canine brain using a 3 T MREIT system: postmortem experiments. Physiol. Meas. 28, 1341–1353.
Kim, H.J., Oh, T.I., Kim, Y.T., Lee, B.I., Woo, E.J., Seo, J.K., Lee, S.Y., Kwon, O., Park, C., Kang, B.T., Park, H.M., 2008. In vivo electrical conductivity imaging of a canine brain using a 3 T MREIT system. Physiol. Meas. 29, 1145–1155.
Konn, D., Gowland, P., Bowtell, R., 2003. MRI detection of weak magnetic fields due to an extended current dipole in a conducting sphere: a model for direct detection of neuronal currents in the brain. Magn. Reson. Med. 50, 40–49.
Kwon, Y.H., Ko, M.H., Ahn, S.H., Kim, Y.H., Song, J.C., Lee, C.H., Chang, M.C., Jang, S.H., 2008. Primary motor cortex activation by transcranial direct current stimulation in the human brain. Neurosci. Lett. 435, 56–59.
Lang, N., Siebner, H.R., Ward, N.S., Lee, L., Nitsche, M.A., Paulus, W., Rothwell, J.C., Lemon, R.N., Frackowiak, R.S., 2005. How does transcranial DC stimulation of the primary motor cortex alter regional neuronal activity in the human brain? Eur. J. Neurosci. 22, 495–504.
Li, C.L., Bak, A.F., Parker, L.O., 1968. Specific resistivity of the cerebral cortex and white matter. Exp. Neurol. 20, 544–557.

Nitsche, M.A., Paulus, W., 2011. Transcranial direct current stimulation–update 2011. Restor. Neurol. Neurosci. 29, 463–492.
Polania, R., Paulus, W., Nitsche, M.A., 2012. Modulating cortico-striatal and thalamo-cortical functional connectivity with transcranial direct current stimulation. Hum. Brain Mapp. 33 (10), 2499–2508.
Reis, J., Fritsch, B., 2011. Modulation of motor performance and motor learning by transcranial direct current stimulation. Curr. Opin. Neurol. 24, 590–596.
Rice, J.K., Rorden, C., Little, J.S., Parra, L.C., 2013. Subject Position Affects EEG Magnitudes. NeuroImage 64C, 476–484. http://dx.doi.org/10.1016/j.neuroimage.2012.09.041.
Salvador, R., Mekonnen, A., Ruffini, G., Miranda, P.C., 2010. Modeling the electric field induced in a high resolution realistic head model during transcranial current stimulation. Conference proceedings: Annual International Conference of the IEEE Engineering in Medicine and Biology Society IEEE Engineering in Medicine and Biology Society Conference 2010, pp. 2073–2076.
Scott, G.C., Joy, M.G., Armstrong, R.L., Henkelman, R.M., 1991. Measurement of nonuniform current density by magnetic resonance. IEEE Trans. Med. Imaging 10, 362–374.
Scott, G.C., Joy, M.L., Armstrong, R.L., Henkelman, R.M., 1992. RF current density imaging in homogeneous media. Magn. Reson. Med. 28, 186–201.
Wendel, K., Malmivuo, J., 2006. Correlation between live and post mortem skull conductivity measurements. Conference proceedings: Annual International Conference of the IEEE Engineering in Medicine and Biology Society IEEE Engineering in Medicine and Biology Society Conference, 1, pp. 4285–4288.
Wojtczyk, H., Graf, H., Martirosian, P., Ballweg, V., Kraiger, M., Pintaske, J., Schick, F., 2011. Quantification of direct current in electrically active implants using MRI methods. Z. Med. Phys. 21, 135–146.
Xiong, J., Fox, P.T., Gao, J.H., 2003. Directly mapping magnetic field effects of neuronal activity by magnetic resonance imaging. Hum. Brain Mapp. 20, 41–49.
Zheng, X., Alsop, D.C., Schlaug, G., 2011. Effects of transcranial direct current stimulation (tDCS) on human regional cerebral blood flow. Neuroimage 58, 26–33.